Analytical Biochemistry **298,** 231–240 (2001)
doi:10.1006/abio.2001.5399, available online at http://www.idealibrary.com on IDEAL®

Synthesis and Fluorescence Characterization of Pteridine Adenosine Nucleoside Analogs for DNA Incorporation

Mary E. Hawkins, Wolfgang Pfleiderer,* Oliver Jungmann,* and Frank M. Balis
*Pediatric Oncology Branch, National Cancer Institute, NIH, Bethesda, Maryland 20892; and *Fakultät für Chemie, Universität Konstanz, Konstanz, Germany*

Received May 14, 2001; published online October 17, 2001

Two fluorescent adenosine analogs, 4-amino-6-methyl-8-(2-deoxy-β-D-ribofuranosyl)-7(8*H*)-pteridone (6MAP) and 4-amino-2,6-dimethyl-8-(2′-deoxy-β-D-ribofuranosyl)-7(8*H*)-pteridone (DMAP), have been synthesized as phosphoramidites. These probes are site-selectively incorporated into oligonucleotides using automated DNA synthesis. Relative quantum yields are 0.39 for 6MAP and 0.48 for DMAP as monomers and range from >0.01 to 0.11 in oligonucleotides. Excitation maxima are 310 (6MAP) and 330 nm (DMAP) and the emission maximum for each is 430 nm. Fluorescence decay curves of each are monoexponential exhibiting lifetimes of 3.8 and 4.8 ns for 6MAP and DMAP, respectively. When these probes are incorporated into oligonucleotides they display quenching of fluorescence intensity, increases in the complexity of decay curves, and decreases in mean lifetimes. Because these changes are apparently mediated by interactions with neighboring bases, spectral changes that occur as probe-containing oligonucleotides meet and react with other molecules provide a means of monitoring these interactions in real time. These probes are minimally disruptive to DNA structure as evidenced by melting temperatures of probe-containing oligonucleotides that are very similar to those of controls. Digestion of probe-containing oligonucleotides with P1 nuclease confirms probe stability as fluorescence levels are restored to those expected for each monomer. These adenosine analog probes are capable of providing information on DNA structure as it responds to binding or catalysis through interaction with other molecules.

Key Words: **DNA; phosphoramidites; pteridine nucleoside analogs.**

Fluorescence is a powerful and sensitive tool for studying the biochemistry of DNA and protein–DNA interactions. Because DNA is inherently only slightly fluorescent, for most studies, highly fluorescent probes with more favorable spectral characteristics, such as fluorescein, are attached to the DNA molecule through a carbon linker. While this attachment makes their presence tolerable, it limits the usefulness of these probes for more subtle measurements. Linker-attached probes are less sensitive to changes occurring within the DNA because of their spatial separation from the DNA. The linker attachment also permits the probe to rotate and move in ways that may be independent of the motion experienced by the DNA. Data from these experiments are often quite complex and may be difficult to interpret.

We have previously described a new class of pteridine-based fluorophores that are chemical analogs of the nucleosides that comprise nucleic acids (1, 2). Of the molecules examined in the previous studies, only 3MI (probe 4) and 6MI (probe 17) have been studied in DNA. 3MI and 6MI are highly fluorescent and are incorporated directly into DNA through a native-like deoxyribose moiety. The availability as phosphoramidites permits these probes to be site selectively incorporated into an oligonucleotide using automated DNA synthesis (1, 2). The fluorescence properties of these fluorophores are markedly altered by their incorporation into an oligonucleotide, and we have developed methods that utilize this feature to study proteins that alter the structure of the DNA (2–4).

The adenosine analogs, probes 1 and 2, from the 1997 study have not been pursued because they contain phenyl groups considered to be potentially obtrusive in a closely base stacked environment. Probe 25 in the series examined in the 1997 study contains no methyl or phenyl groups and was a very attractive adenosine analog; however, this probe proved to be unstable as evidenced by loss in fluorescence intensity during spectral analysis. The synthesis and fluores-

0003-2697/01 $35.00

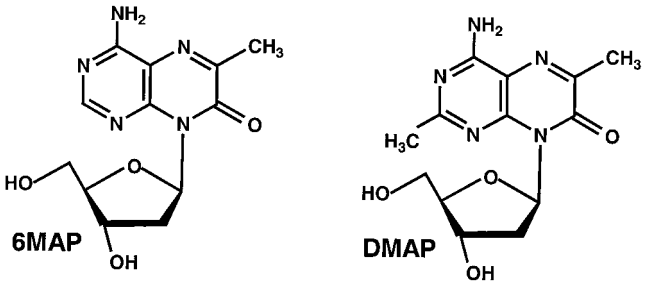

FIG. 1. The structures of 6MAP and DMAP.

cence properties of two new pteridine-based adenosine analogs (Fig. 1), 4-amino-6-methyl-8-(2-deoxy-β-D-ribofuranosyl)-7(8*H*)-pteridone (6MAP)[1] and 4-amino-2,6-dimethyl-8-(2′-deoxy-β-D-ribofuranosyl)-7(8*H*)-pteridone (DMAP), are described here. These probes were modeled after probes 1 and 2 (1) by replacing the phenyl groups with methyl groups. These adenosine analogs exhibit properties similar to those of the guanosine analogs, 3MI and 6MI, for which there are numerous applications (2–4) and will extend our options in situations requiring an adenosine analog.

MATERIALS AND METHODS

Chemicals

The steps in the synthesis of 6MAP and DMAP and their phosphoramidite forms are shown in Fig. 2 and described in detail below. Odd-numbered compounds are for 6MAP synthesis and even-numbered compounds are for DMAP synthesis.

4-Amino-6-methyl-8-[2-deoxy-5-O-(4,4′-dimethoxytrityl)-β-D-ribofuranosyl]-7(8H)-pteridone-3′-O-(H-β-cyanoethyl-N-diisopropyl)phosphoramidite

Step 1: Synthesis of 4-amino-6-methyl-7(8H)-pteridone (compound 3) (6). Two grams (16 mmol) of 4,5,6-triaminopyrimidine (compound 1) (7) and 2.2 ml of ethyl pyruvate (19 mmol) were heated under reflux in 20 ml of glacial acetic acid for 2 h. After cooling, the precipitate was collected, washed with water, and purified by recrystallization from 350 ml of a 1:1 (v/v) solution of dimethylformamide (DMF)/water. The yield was 1.25 g (44%); the melting point (m.p.) of the product was >360°C; the λ_{max} (log ϵ) (pH 5) for each peak from the UV absorbance scan were 218 (4.37), 243 (4.07), [291 (3.82)], 326 (4.02), and [343 (3.89)]; and the ^{1}H NMR (D_6-DMSO) spectrum results were 2.34 (s, CH_3-C(6)), 7.35 + 7.45 (2 bs, NH_2); 8.12 (s, H-C(2)), 12.56 (bs, H-N(8)).

Step 2: Synthesis of 4-amino-6-methyl-8-(2-deoxy-3,5-di-O-p-chlorobenzoyl-β-D-ribofuranosyl)-7(8H)-pteridone (compound 5). A total of 1.54 g (9 mmol) of compound 3 and 1.34 ml (9 mmol) of 1,8-diazabicyclo-[5.4.0]undec-7-ene (DBU) were stirred in 100 ml anhydrous acetonitrile for 30 min. A total 4.46 g (10.8 mmol) 2-deoxy-3,5-di-*O*-*p*-chlorobenzoyl-α-D-ribofuranosyl chloride (8) was added, and the mixture was stirred for 2 h and then evaporated. The residue was dissolved in 60 ml of dichloromethane and washed twice with a saturated solution of NaCl (30 ml each). The organic layer was then dried over Na_2SO_4, filtered, and evaporated. The crude product was dissolved in 10 ml of toluene, applied to a silica gel column (5 × 11 cm), washed with 600 ml of 2:1 (v/v) solution of toluene and ethyl acetate, and then eluted with 400 ml of a 1:1 (v/v) toluene and ethyl acetate solution. The main fraction was evaporated and then recrystallized from a 2:1 (v/v) $CHCl_3$/methanol solution to yield 1.7 g (34%) of colorless crystals. m.p. >187–189°C; UV λ_{max} (log ϵ) (methanol), 241 (4.66), 333 (3.96); ^{1}H NMR (D_6-DMSO), 2.38 (s, CH_3-C(6)), 2.55 (m, H_α-C(2′)), 3.18 (m, H_β-(2′)), 4.53 (m, 2 H-C(5′)), 4.69 (m, H-C(4′)), 5.94 (m, H-C(3′)), 7.34 (m, H-C(1′)), 7.51 (d, 2H *p*-chlorobenzoyl), 7.59 (d, 2H *p*-chlorobenzoyl), 7.79 (bs, NH_2), 7.93 (2d, 4H *p*-chlorobenzoyl), 8.22 (s, H-C(2)). Analysis for $C_{26}H_{21}Cl_2N_5O_6$ (MW, 570.4): calculated, C 54.75, H 3.71, N 12.28; found, C 54.52, H 3.80, N 12.28.

Step 3: Synthesis of 4-amino-6-methyl-8-(2-deoxy-β-D-ribofuranosyl)-7(8H)-pteridone (compound 7). A total of 0.5 g (0.88 mmol) of compound 5 was added to a solution of sodium (20 mg) in 20 ml anhydrous methanol and stirred at room temperature for 12 h. After neutralization with acetic acid, the suspension was concentrated to 10 ml. The precipitate was collected, washed with methanol, and dried in high vacuum to yield 0.16 g (62%). Cooling of the filtrate provided a second crop of 0.05 g (19%). m.p. >190°C decomposition; UV λ_{max} (log ϵ) (methanol), 248 (4.09), [292 (3.71)], and 329 (3.93); ^{1}H NMR (D_6-DMSO), 2.01 (m, H_α-C(2′)), 2.36 (s, Me), 2.88 (m, H_β-C(2′)), 3.54 (m, H-C(5′)), 3.60 (m, H-C(5″)), 3.67 (m, H-C(4′)), 4.44 (m, H-C(3′)), 4.72 (dd, HO-C(5′)), 5.17 (d, HO-C(3′)), 7.15 (m, H-C(1′)), 7.52 + 7.70 (2s, NH_2), 8.20 (s, H-C(2)). Analysis for $C_{12}H_{15}N_5O_4$ (MW, 293.3): calculated, C 49.13, H 5.16, N 23.88; found, C 49.34, H 5.18, N 23.78.

Step 4: Synthesis of 4-amino-6-methyl-8-[2-deoxy-5-O-(4,4′-dimethoxytrityl)-β-D-ribofuranosyl]-7(8H)-pteridone (compound 9). A total of f1.25 g (4.26 mmol) of compound 7 was coevaporated twice with 20 ml of anhydrous pyridine and then dissolved in 20 ml of the same solvent. A total of 1.73 g (5.1 mmol) of 4,4′-dimethoxytrityl chloride was added and stirred at room temper-

[1] Abbreviations used: 6MAP, 4-amino-6-methyl-8-(2-deoxy-β-D-ribofuranosyl)-7(8*H*)-pteridone; DMAP, 4-amino-2,6-dimethyl-8-(2′-deoxy-β-D-ribofuranosyl)-7(8*H*)-pteridone; DMF, dimethylformamide; m.p., melting point; DMSO, dimethyl sulfoxide; DBU, 1,8-diazabicyclo-[5.4.0]undec-7-ene; DAS, decay-associated spectra.

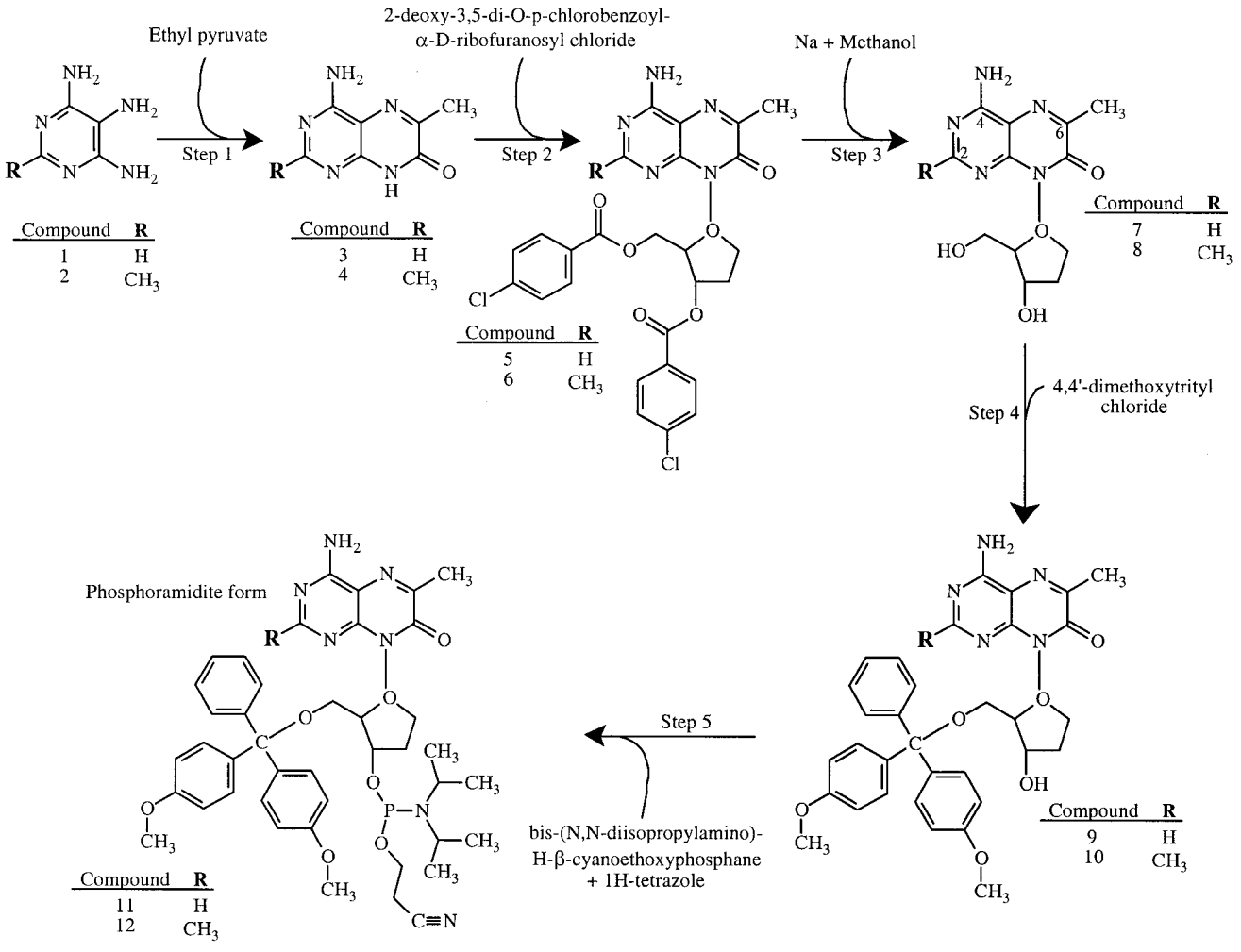

FIG. 2. Synthetic scheme for 6MAP and DMAP.

ature for 12 h. After evaporation, the residue was dissolved in 40 ml of CH_2Cl_2 and washed twice with 20 ml of saturated $NaHCO_3$ solution. The organic phase was dried over Na_2SO_4 and evaporated. The residue was dissolved in 5 ml of toluene, applied to a silica gel column (12 × 5 cm), and washed with 400 ml of 1:3 (v/v) toluene:ethyl acetate and eluted with 600 ml of 1:1 (v/v) toluene:ethyl acetate. The product fraction was evaporated and the resulting solid foam was dried in high vacuum to yield 2.16 g (85%). m.p. >90–105°C; UV λ_{max} (log ϵ) (methanol), [233 (4.52)], [278 (3.84)], and 328 (3.94); ^{1}H NMR (D_6-DMSO), 2.11 (m, H_α-C(2′)), 2.30 (s, CH_3-C(6′)), 2.78 (m, H_β-C(2′)), 3.15 (m, H-C(5′)), 3.33 (m, H-C(5″)), 3.69 (s, OCH_3), 3.70 (s, OCH_3), 3.94 (m, H-C(4′)), 4.44 (m, H-C(3′)), 5.17 (d, OH-C(3′)), 6.77 (2d, 4H, trityl), 7.20 (m, 7H, trityl), 7.35 (m, 2H, trityl), 7.50 + 7.67 (2 bs, NH_2), 8.11 (s, H-C(2)). Analysis for $C_{33}H_{33}N_5O_6$ (MW, 595.7): calculated, C 66.54, H 5.58, N 11.76; found, C 66.58, H 5.92, N 11.73.

Step 5: Synthesis of 4-amino-6-methyl-8-[2-deoxy-5-O-(4,4′-dimethoxytrityl)-β-D-ribofuranosyl] 7(8H)-pteridone-3′-O-(H-β-cyanoethyl N-diisopropyl)phosphoramidite (compound 11). A total of 1.25 g (2.1 mmol) of compound 9, 0.95 g (3.1 mmol) of bis-(*N,N*-diisopropylamino)-*H*-β-cyanoethoxyphosphane and 74 mg (1.05 mmol) of 1-*H*-tetrazole were dissolved in 30 ml of anhydrous CH_2Cl_2 and stirred at room temperature under nitrogen atmosphere for 12 h. The solution was diluted with 10 ml of CH_2Cl_2 and washed twice with 10-ml aliquots of a saturated $NaHCO_3$ solution. The organic phase was then dried over Na_2SO_4 and evaporated. The resulting solid foam was dissolved in 3 ml of toluene, applied to a silica gel column (12 × 5 cm), and eluted with 500 ml of 1:1 (v/v) toluene:ethyl acetate containing a few drops of triethylamine. The product fraction was evaporated to yield 1.46 g (86%) of a solid colorless foam. m.p. >70–75°C; UV (methanol), [233 (4.49)], [278 (3.81)], 328 (3.91); ^{1}H NMR (D_6-DMSO), 0.92–1.07 (m, 2 CH(CH_3)$_2$), 2.29 (s, CH_3-C(6)), 2.30 (m,

H_{α}-C(2′)), 2.59 (t, OCH_2CH_2CN), 2.85 (m, H_{β}-C(2′)), 3.12 (m, H-C(5′)), 3.27 (m, H-C(5″)), 3.38–3.57 (m, 2 $CH(CH_3)_2$, OCH_2CH_2CN)), 3.68 (s, 2 OCH_3), 4.06 (m, H-C(4′)), 4.71 (m, H-C(3′)), 6.76 (m, 4H, trityl), 7.19 (m, 7H, trityl, H-C(1′)), 7.33 (m, 2H, trityl), 7.51 + 7.68 (2 bs, NH_2), 8.09 (s, H-C(2)). Analysis for $C_{42}H_{50}N_7O_7P$ (795.9): calculated, C 63.38, H 6.33, N 12.32; found, C 63.62, H 6.39, N 11.84.

4-Amino-2,6-dimethyl-8-[2-deoxy-5-O-(4,4′-dimethoxytrityl)-β-D-ribofuranosyl]-7(8H)-pteridone-3′-O-(H-β-cyanoethyl N-diisopropyl)phosphoramidite

Step 1: Synthesis of 4-amino-2,6-dimethyl-7(8H)-pteridone (compound 4). A total of 0.5 g (3.6 mmol) of 4,5,6-triamino-2-methylpyrimidine (compound 2) (5) and 1 ml of ethyl pyruvate were heated in 20 ml of 1:1 (v/v) acetic acid:ethanol under reflux for 1 h. After cooling, the precipitate was collected and recrystallized from 90 ml of 1:1 (v/v) DMF/H_2O with charcoal yielding 0.372 g (54%) of colorless crystals. m.p. >300°C (decomposition); UV λ_{max} (log ϵ) (pH 5), 245 (4.08), [291 (3.77)], [318 (4.00)], 331 (4.03), [345 (3.88)]; ^{1}H NMR (D_6-DMSO), 2.34 (s, 6H, CH_3-C(2), CH_3-C(6)), 7.32 + 7.42 (2 bs, NH_2), 12.43 (bs, H-N(8)). Analysis for $C_8H_9N_5O$ (MW, 190.1): calculated, C 50.26, H 4.74, N 36.63; found, C 50.15, H 4.82, N 36.35.

Step 2: Synthesis of 4-amino-2,6-dimethyl-8-(2-deoxy-3,5-di-O-p-chlorobenzoyl-β-D-ribofuranosyl)-7(8H)-pteridone (compound 6). A total of 1.58 g (8.26 mmol) of compound 4 was suspended in 60 ml of anhydrous acetonitrile, 1.23 ml of DBU (8.26 mmol) was added, and the solution was stirred for 15 min at room temperature. After adding 4.2 g (10 mmol) of 2-deoxy-3,5-di-*O*-*p*-chlorobenzoyl-β-D-ribofuranosyl chloride, the mixture was stirred for 2 h. The colorless precipitate was collected and recrystallized from 90 ml 1:2 (v/v) $CHCl_3$/methanol, yielding 1.92 g (40%). m.p. >218–220°C (decomposition); UV λ_{max} (log ϵ) (methanol), 241 (4.66), 333 (3.96); ^{1}H NMR (D_6-DMSO), 2.36 (s, CH_3-C), 2.40 (s, CH_3-C), 2.57 (m, H_{α}-C(2′)), 3.17 (m, H_{β}-C(2′)), 4.53 (m, 2 H-C(5′)), 4.69 (m, H-C(4′)), 6.00 (m, H-C(3′)), 7.30 (m, H-C(1′)), 7.42 (bs, NH_2), 7.50 (d, 2H *p*-chlorobenzoyl), 7.59 (d, 2H *p*-chlorobenzoyl), 7.89 (d, m2H *p*-chlorobenzoyl), 7.96 (d, 2H *p*-chlorobenzoyl). Analysis for $C_{27}H_{23}Cl_2N_5O_6$ (MW, 548.4): calculated, C 55.49, H 3.97, N 11.98; found, C 55.57, H 4.09, N 11.53.

Step 3: Synthesis of 4-amino-2,6-dimethyl-8-(2-deoxy-β-D-ribofuranosyl)-7(8H)-pteridone (compound 8). A total of 0.78 g (1.33 mmol) of compound 6 was added to a solution of 30 mg of sodium in 20 ml of anhydrous methanol and stirred at room temperature for 12 h. After neutralization with acetic acid and concentration to 10 ml, the precipitate was collected, washed with methanol, and dried in high vacuum to yield 0.38 g (93%) of colorless crystals. m.p. >180°C (decomposition); UV λ_{max} (log ϵ) (methanol), 250 (4.08), [298 (3.74)], 333 (3.95); ^{1}H NMR (D_6-DMSO), 1.99 (m, H_{α}-C(2′)), 2.34 (s, CH_3), 2.37 (s, CH_3), 2.88 (m, H_{β}-C(2′)), 3.53 (m, H-C(5′)), 3.65 (m, H-C(5″)), 3.74 (m, H-C(4′)), 4.45 (m, H-C(3′)), 4.66 (dd, HO-C(5′)), 5.16 (d, HO-C(3′)), 7.14 (m, H-C(1′)), 7.38 + 7.57 (2s, NH_2). Analysis for $C_{13}H_{17}N_5O_4$ (MW, 307.3): calculated, C 50.81, H 5.58, N 22.79; found, C 50.34, H 5.80, N 23.08.

Step 4: Synthesis of 4-amino-2,6-dimethyl-8-[2-deoxy-5-O-(4,4′-dimethoxytrityl)-β-D-ribofuranosyl]-7(8H)-pteridone (compound 10). A total of 0.57 g (1.85 mmol) of compound 8 was coevaporated twice with 10 ml of anhydrous pyridine and then dissolved in 15 ml of the same solvent. A total of 0.752 g (2.22 mmol) of 4,4′-dimethoxytrityl chloride was added and the solution was stirred at room temperature for 12 h. After evaporation, the residue was dissolved in 20 ml of CH_2Cl_2 and washed twice with 20 ml of saturated $NaHCO_3$ solution. The organic phase was dried over Na_2SO_4 and evaporated. The residue was dissolved in 5 ml of toluene, applied to a silica gel column, washed with 300 ml of 1:1 (v/v) toluene:ethyl acetate, and then eluted with 200 ml of 1:3 (v/v) toluene:ethyl acetate. The product was evaporated and the resulting solid foam was dried in high vacuum yielding 0.785 g (70%). m.p. >105–120°C; UV λ_{max} (log ϵ) (methanol), [232 (4.46)], [258 (4.11)], 333 (3.96); ^{1}H NMR (D_6-DMSO), 2.08 (m, H_{α}-C(2′)), 2.18 (s, CH_3-C(6)), 2.29 (s, CH_3-C(6)), 2.76 (m, H_{β}-C(2′)), 3.12 (m, H-C(5′)), 3.39 (m, H-C(5″)), 3.68 (s, OCH_3), 3.70 (s, OCH_3), 3.94 (m, H-C(4′)), 4.45 (m, H-C(3′)), 5.16 (d, OH-C(3′)), 6.78 (2d, 4H, trityl), 7.17 (m, 7H, trityl), 7.33 (m, 2H, trityl), 7.34 + 7.67 (2 bs, NH_2). Analysis for $C_{33}H_{33}N_5O_6 \times H_2O$ (MW, 627.7): calculated, C 65.06, H 5.94, N 11.16; found, C 64.92, H 5.92, N 11.23.

Step 5: Synthesis of 4-amino-2,6-dimethyl-8-[2-deoxy-5-O-(4,4′-dimethoxytrityl)-β-D-ribofuranosyl]-7(8H)-pteridone-3′-O-(H-β-cyanoethyl N-diisopropyl)-phosphoramidite (compound 12). A total of 0.61 g (1 mmol) of compound 10, 0.45 g (1.5 mmol) of bis-(*N,N*-diisopropylamino)-*H*-β-cyanoethoxyphosphane, and 35 mg (0.5 mmol) of 1*H*-tetrazole were dissolved in 15 ml of anhydrous CH_2Cl_2 and stirred at room temperature under nitrogen atmosphere for 12 h. This mixture was then was diluted with 10 ml of CH_2Cl_2 and washed twice with 10 ml of a saturated $NaHCO_3$ solution, and then the organic phase was dried over Na_2SO_4 and evaporated. The solid foam was dissolved in 5 ml of toluene, applied to a silica gel column (12 × 1.5 cm), and eluted with 150 ml of 3:2 (v/v) toluene:ethyl acetate containing a few drops of triethylamine. The product fraction was evaporated to yield 0.69 g (85%) of solid colorless foam. UV λ_{max} (log ϵ) (methanol), [231 (4.48)], [258 (4.13)], 334 (3.95); ^{1}H NMR (D_6-DMSO), 0.88–1.01

(m, 2 CH(CH_3)$_2$), 2.29 (s, CH_3-C(2)), 2.30 (s, CH_3-C(6)), 2.30 (m, H_α-C(2′)), 2.59 (t, OCH_2CH_2CN), 2.83 (m, H_β-C(2′)), 3.11 (m, H-C(5′)), 3.25 (m, H-C(5″)), 3.38–357 (m, 2 CH(CH_3)$_2$, OCH_2CH_2CN), 3.69 (s, 2 OCH_3), 4.10 (m, H-C(4′)), 4.73 (m, H-C(3′)), 6.75 (m, 4H, trityl), 7.19 (m, 7H, trityl), H-C(1′)), 7.33 (m, 2H, trityl), 7.33 + 7.54 (2 bs, NH_2). Analysis for $C_{43}H_{52}N_7O_7P$ (MW, 809.9): calculated, C 63.77, H 6.47, N 12.11; found, C 63.70, H 6.50, N 12.01.

Oligonucleotide Synthesis and Purification

6MAP and DMAP were incorporated directly into oligonucleotides and purified following procedures detailed previously (2). Double-stranded oligonucleotides were formed by combining complementary strands at equimolar concentrations, heating to >85°C, and allowing the mixture to cool to room temperature. For comparison of fluorescence intensity of double- to single-stranded fluorophore-containing oligonucleotides, an excess of non-fluorophore-containing complementary oligonucleotide strand was added to ensure that all of the fluorophore-containing strands were annealed.

Melting temperatures of double-stranded oligonucleotides were obtained by methods reported previously (1).

Spectroscopic Analysis

Fluorescence was measured on a PTI (Photon Technologies, Inc., New Brunswick, NJ) spectrofluorometer equipped with a 75-W xenon arc lamp, a double excitation monochrometer, and a water-cooled photomultiplier. The spectrofluorometer was interfaced with a Pharmacia Multitemp LKB water bath temperature controller (Pharmacia). Small volume samples were measured in 3 × 3-mm quartz cuvettes supported by custom built adapters. Relative quantum yields were measured as reported previously (2) A Hewlett–Packard Model 8452a spectrophotometer (Palo Alto, CA) was used for UV-VIS analysis. Lifetime estimates were derived as reported previously (1). For decay-associated spectra (DAS), time-resolved data were obtained on samples by excitation at 330 nm and observation every 5 nm over the emission band. The excitation pulse ("lamp") profile was obtained with a light-scattering suspension (Ludox) from Sigma. Further instrumentation details were reported previously (1). DAS are the emission spectra that belong to each lifetime obtained from fluorescence decay surfaces and are used to dissect the heterogeneity of the emission but do not, in themselves, specify its origin. The lifetimes are obtained by global analysis of the entire surface. The DAS are viewed as plots of the preexponential constants (α_I) at each wavelength, and these spectra can be normalized to provide the intensity contribution from each component.

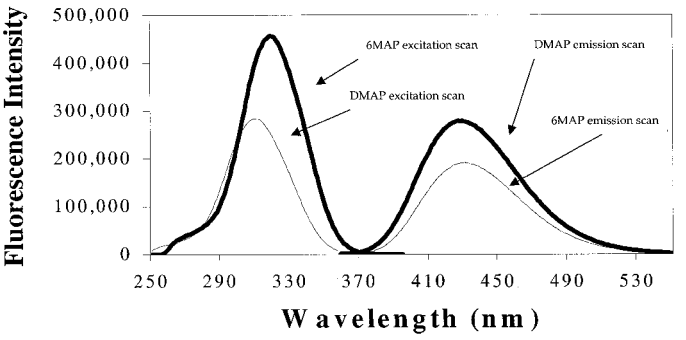

FIG. 3. Excitation (250–400 nm) and emission (365–540 nm) scans of 6MAP (bold lines) and DMAP (fine lines). Samples were measured in 10 mM Tris, pH 7.5, at room temperature.

P1 Nuclease Digestion

Fluorophore-containing oligonucleotides were digested with 3 Units of *Penicillium citrinum* P1 nuclease (Boehringer Mannheim Biochemica) in a total volume of 100 μl. A fluorescence scan of the intact oligonucleotide was compared to the fluorescence scan of the digest that was generated after incubation of the mixture at 37°C for 19 h. The ratio of these two scans was compared to the ratio of the relative quantum yields of the oligonucleotide substrate and the monomer form of 6MAP and DMAP.

RESULTS

Fluorescence of 6MAP and DMAP Monomers

The excitation wavelength maxima for 6MAP and DMAP in their monomer form were 320 and 310 nm, respectively, and the emission wavelength maximum was 430 nm for each fluorophore (Fig. 3). The relative quantum yields (Q_{rel}) of 6MAP and DMAP were 0.39 and 0.48, respectively. Lifetimes for 6MAP and DMAP in monomer form were 3.8 and 4.8 ns, respectively, and DAS for each compound exhibited one main component (>98%). Each probe was found to be stable in ambient light and at room temperature for >24 h.

Fluorescence of 6MAP- or DMAP-Containing Oligonucleotides

Incorporation of 6MAP and DMAP into an oligonucleotide substantially quenched fluorescence. The Q_{rel} of 6MAP-containing oligonucleotides (numbered 21–29) were ranged from <0.01 to 0.041 and the Q_{rel} of DMAP-containing oligonucleotides (numbered 31–39)

TABLE 1

Sequences Containing 6MAP or DMAP and Relative Quantum Yields (Q_{rel})

Sequence (5′ → 3′)	6MAP in F Position		DMAP in F Position	
	Name	Q_{rel}	Name	Q_{rel}
gtg tgg **F**aa atc tct agc agt	PTR21	0.010	PTR31	0.023
gtg tgg aaa **F**tc tct agc agt	PTR22	0.020	PTR32	0.022
gtg tgg aaa atc tct **F**gc agt	PTR23	0.018	PTR33	0.01
act gct **F**ga gat ttt cca cac	PTR24	—	PTR34	0.012
act gct ag**F** gat ttt cca cac	PTR25	0.011	PTR35	0.017
act gct aga g**F**t ttt cca cac			PTR36	0.019
act gct aga gat ttt cc**F** cac	PTR27	—	PTR37	0.11
act gct agc c**F**t ttt cca cac	PTR28	0.041	PTR38	0.11
att cca caa **F**gc cgt gtc a	HP21	0.010	HP31	0.02
aga ggt gtc c**F**c ctg tgg aga	HP22	<0.01	HP32	<0.01
aga ggt gta c**F**a gtg tgg aga	HP23	0.012	HP33	0.02
aga ggt gta a**F**a atg tgg aga	HP24	<0.01	HP34	<0.01

ranged from <0.01 to 0.11 (Table 1). In general, oligonucleotides in which the fluorophore is surrounded by pyrimidines (such as PTR28 and PTR38) were less severely quenched than oligonucleotides in which the fluorophore is adjacent to a purine (such as HP24 and HP34).

The lifetimes, mean lifetimes, and amplitudes for 6MAP- and DMAP-containing single-stranded oligonucleotides are listed in Table 2. The fluorescence decay curves of the fluorophore-containing oligonucleotides were more complex than the monoexponential curves of the monomers, and the dominant component of the intensity decay curves of the oligonucleotides for both fluorophores have shorter lifetimes (τ_i) than the monomer form. The mean intensity-weighted and species-concentration-weighted lifetimes (τ_m and $<\tau>$) for the fluorophore-containing oligonucleotides were also shorter than the lifetimes of the monomers.

TABLE 2

Fluorescence Properties of 6MAP- and DMAP-Containing Oligonucleotides (Sequences Shown in Table 1)

Sequence	fluorophore	Q_{rel}[a]	τ_i (ns)	α_i	%I	τ_m (ns)	$\langle\tau\rangle$ (ns)
PTR21	6MAP	0.010	$\tau_1 = 0.69$	$\alpha_1 = 0.30$	9.6	2.58	2.15
			$\tau_2 = 2.78$	$\alpha_2 = 0.70$	90.4		
PTR25	6MAP	0.011	$\tau_1 = 2.93$				
PTR27	6MAP		$\tau_1 = 0.29$	$\alpha_1 = 0.40$	9.2	2.26	1.26
			$\tau_2 = 1.54$	$\alpha_2 = 0.53$	64.6		
			$\tau_3 = 4.73$	$\alpha_3 = 0.07$	26.2		
PTR28	6MAP	0.041	$\tau_1 = 0.17$	$\alpha_1 = 0.38$	5.9	1.82	1.09
			$\tau_2 = 1.15$	$\alpha_2 = 0.40$	42.3		
			$\tau_3 = 2.56$	$\alpha_3 = 0.22$	51.8		
HP21	6MAP	0.010	$\tau_1 = 0.69$	$\alpha_1 = 0.41$	13.1	2.85	2.16
			$\tau_2 = 3.18$	$\alpha_2 = 0.59$	86.9		
HP22	6MAP	<0.010	$\tau_1 = 0.61$	$\alpha_1 = 0.52$	17.5	2.68	1.81
			$\tau_2 = 3.12$	$\alpha_2 = 0.48$	82.5		
HP23	6MAP	0.012	$\tau_1 = 0.48$	$\alpha_1 = 0.59$	21.1	2.13	1.34
			$\tau_2 = 2.58$	$\alpha_2 = 0.41$	78.9		
PTR32	DMAP	0.022	$\tau_1 = 0.40$	$\alpha_1 = 0.39$	8.1	2.7	1.92
			$\tau_2 = 2.90$	$\alpha_2 = 0.61$	91.9		
PTR38	DMAP	0.11	$\tau_1 = 0.77$	$\alpha_1 = 0.42$	16.6	2.46	1.95
			$\tau_2 = 2.80$	$\alpha_2 = 0.58$	83.4		
HP33	DMAP	0.020	$\tau_1 = 0.28$	$\alpha_1 = 0.65$	17.1	2.14	1.06
			$\tau_2 = 2.52$	$\alpha_2 = 0.35$	82.9		

[a] Abbreviations: Q_{rel}, relative quantum yield; τ_i, lifetime for each component of a multiexponential model; α_i, preexponential for each component of a multiexponential model; %I, percentage of fluorescence intensity for each component of a multiexponential model; $\langle\tau\rangle$, species-concentration-weighted lifetime; τ_m, intensity-weighted lifetime.

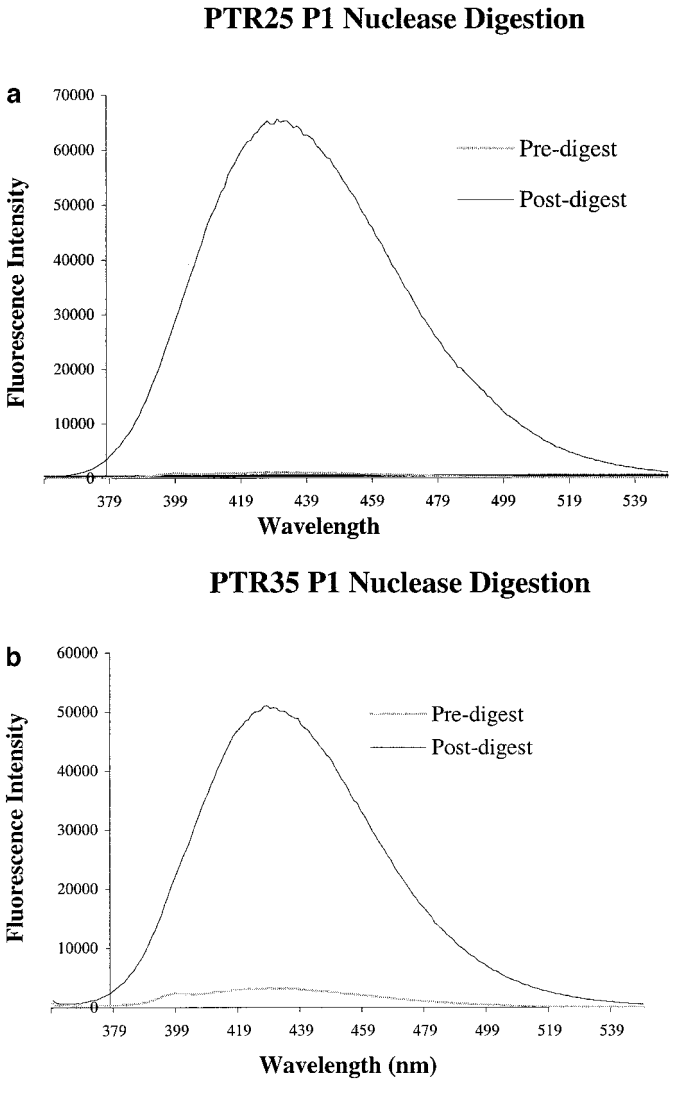

FIG. 4. Emission scan of a single-stranded probe-containing oligonucleotide before (dotted line) and after (solid line) digestion by P1 nuclease. Reactions were carried out at 37°C for 16 h in 100 μl volume.

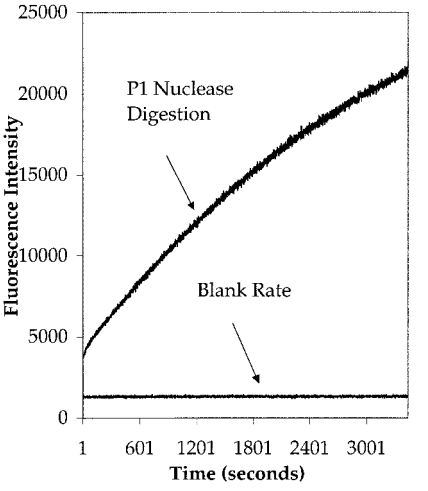

FIG. 5. P1 nuclease digestion in real time as measured in the time-based acquisition mode. The blank rate contains all the same components with the exception of P1 nuclease.

P1 Nuclease Digestion of 6MAP- or DMAP-Containing Single-Stranded Oligonucleotides

6MAP- and DMAP-containing single-stranded oligonucleotides were subjected to P1 nuclease digestion in order to establish that the substantial decrease in fluorescence intensity after incorporation into the oligonucleotide was from quenching and not from degradation of the fluorophores during DNA synthesis. Digestion of fluorophore-containing oligonucleotides resulted in a marked increase in fluorescence intensity (Fig. 4). For each fluorophore, the ratio of the fluorescence emission scan of predigested oligonucleotide to the fluorescence emission scan of the digested product was equivalent to the ratio of the quantum yield of the 6MAP- or DMAP-containing single-stranded oligonucleotide to the quantum yield of the monomer form. This demonstrates that the fluorophores can be recovered intact from the oligonucleotide and that the decrease in fluorescence intensity of the fluorophores within the oligonucleotide is related to quenching of the fluorescence signal. Figure 5 displays the real-time data acquisition of fluorescence intensity increase as the probe-containing oligonucleotide is digested by P1 nuclease.

T_m's of 6MAP- or DMAP-Containing Oligonucleotides

T_m's for double-stranded oligonucleotides containing either 6MAP or DMAP paired with thymidine in the complementary strand are shown in Table 3. The T_m's of the DMAP-containing oligonucleotides were de-

TABLE 3

Melting Temperatures for Double-Stranded Oligonucleotides (Sequences Shown in Table 1) Containing 6MAP and DMAP Paired to Thymidine in the Complementary Strand

Sequence	Fluorophore	T_m (°C)
PTR21	6MAP	56.1
PTR22	6MAP	53.5
PTR23	6MAP	54.8
PTR24	6MAP	57.2
PTR25	6MAP	55.3
PTR31	DMAP	52.4
PTR32	DMAP	51.8
PTR33	DMAP	53.8
PTR34	DMAP	54.6
PTR35	DMAP	57.0
PTR36	DMAP	51.6
PTR37	DMAP	51.0
Control	—	57.8

TABLE 4

Melting Temperatures for Oligonucleotides Containing 6MAP or DMAP Paired with Complementary Strands with Substitutions of T, A, C, or G as Pairing Partner for the Fluorophore

		Fluorophore pairing partner (°C)			
Sequence	Fluorophore	T	A	C	G
PTR22	6MAP	53.5	43.8	42.8	45.2
PTR32	DMAP	51.8	45.2	45.6	46.8

Note. See Table 1 for sequences.

pressed to a greater extent than the oligoncleotides containing 6MAP in the identical position. The slight depression of the T_m, compared to the control double-stranded oligonucleotide that did not contain a fluorophore, indicates that the presence of a single 6MAP or DMAP at various positions in one of the strands did not significantly effect annealing of the complementary strands. When adenine, guanine, or cytosine were substituted for thymidine as the pairing partner for the 6MAP and DMAP in the complementary strand the T_m's were depressed to a greater extent (Table 4).

DISCUSSION

Chemical Synthesis

A large number of pteridine nucleosides (6) have been synthesized using the Hilbert–Johnson–Birkofer method (7, 8) which is based on a trimethylsilylation of the heterocycle, followed by glycosylation under catalysis with various Lewis acids (9). A simpler procedure has recently been developed by dissolving the 7(8*H*)-pteridones in acetonitrile utilizing DBU as a base. Subsequent treatment with a halo-sugar (10), such as 2-deoxy-3,5-di-*O*-*p*-chloropbenzoyl-α-D-ribofuranosyl chloride, resulted in a highly stereoselective manner to the corresponding N^8-(2-deoxy-β-ribofuranosides) in good yield. This versatile approach worked very well for 4-amino-6-methyl-(compound 3) and 4-amino-2,6-dimethyl-7(8*H*)pteridone (compound 4), to give the corresponding 2′-deoxyribonucleosides, compounds 5 and 6, respectively, either by normal chromatographic workup or by simple recrystallization. Deprotection of compounds 5 and 6 at the sugar moiety to compounds 7 and 8 was achieved following the Zemplen method (11) which utilizes catalytic amounts of sodium methoxide in methanol. Dimethoxytritylation at the 5′-OH group was achieved in the usual manner by reaction of dimethoxytrityl chloride in pyridine to give compounds 9 and 10 in 85 and 70% yield, respectively. The final conversion to the 3′-*O*-phosphoramidites of compounds 11 and 12 worked very well with bis-(*N*,*N*-diisopropylamino)-β-cyanoethoxyphosphane and tetrazole in the conventional manner to give yields of 85%.

Fluorescence of 6MAP and DMAP Monomers

6MAP and DMAP differ only in the presence of a second methyl group at the 2-postion for DMAP (Fig. 1). Synthesis of an adenosine analog without a methyl group at either the 6- or the 2-position (probe 25), explored previously (1), resulted in an unacceptably labile compound. Because there is not a notable difference (based on spectroscopic analysis of fluorescence intensity) between the stability of 6MAP and DMAP, the presence of the 6-position methyl appears to be sufficient to stabilize the molecules. 6MAP is structurally identical to probe 2 (1) except for the substitution of a methyl group for a phenyl group in the 6-position. A comparison of the relative quantum yields between probe 2 (0.16) and 6MAP (0.38) shows that quenching associated with the phenyl moiety is more severe than that associated with the methyl moiety.

The relative quantum yields of these monomers are quite high, 0.38 and 0.47 for 6MAP and DMAP, respectively. Both 6MAP and DMAP exhibited monoexponential decay in the lifetime measurement, an indication that they exist in a relatively homogeneous environment.

Fluorescence of 6MAP- or DMAP-Containing Oligonucleotides

Fluorescence quenching of the probes as they are positioned within various environments in oligonucleotides is quite complex (Table 1). The patterns of quenching are not as obvious for 6MAP and DMAP as they are for 3MI and 6MI (1, 2). In general, the adenosine analogs (6MAP and DMAP) are much more heavily quenched than the guanosine analogs (3MI and 6MI) within a given oligonucleotide environment. The adenosine analogs do not seem to be consistently affected by proximal purines. For example, HP22 and HP32 both have relative quantum yields below 0.01 and if they were to follow the trend seen with the guanosine analogs, the neighboring pyrimidine environment would yield a relatively brighter signal. The range of relative quantum yields is much smaller with 6MAP (0.04 to $<$0.01) and DMAP (0.11 to $<$0.01) than that seen with 3MI (0.3 to $<$0.01) and that also makes it more difficult to discern a quenching pattern. What is clear, however, is that the adenosine analogs are more heavily quenched within an oligonucleotide than the guanosine analogs. In most cases with either 6MAP or DMAP, additional quenching associated with annealing was less than 2% (compared to monomer fluorescence quantum yield). Since most of these oligonucleotides are already severely quenched in the single

strand (>95%) this is not surprising. In only two cases, PTR37 and PTR38 containing DMAP, the additional quench seen after annealing amounted to substantial increases (20 and 7.5%, respectively).

The range of quantum yields measured for these two probes within oligonucleotides can easily be detected and monitored using a standard bench-top fluorometer. The evidence seen with 3MI-containing oligonucleotides demonstrates that these probes can easily be measured in the oligonucleotide environment (2–4). Highly quenched oligonucleotide-contained probe can be an advantage in experiments where an increase in fluorescence intensity is the indicator for any event that distorts the tertiary structure of the DNA.

Lifetime analysis may provide some insights into quenching or energy transfer effects for these probes. The monomer forms of 6MAP and DMAP display monoexponential decay curves and in most cases, incorporation into an oligonucleotide results in an increase in complexity of the decay curves requiring two and sometimes three components to achieve an acceptable fit. This increase in complexity combined with the impact of severe decreases in $<\tau>$ (43 to 78%) is an indication of the degree of association of the pteridine analogues with the DNA. By comparing changes in fluorescence to changes in lifetimes $<\tau>$, we can learn something about the nature of the quenching mechanism. Static quench will not be accompanied by decreases in $<\tau>$, and purely dynamic quench will exhibit proportional changes in the quantum yield and $<\tau>$. Anything in between these two extremes would suggest that the mechanism of quenching be due to a combination of static and dynamic forces. An example of dynamic quenching is the collisional events from the surroundings (solvent) while an example of static quenching is contact with the sugar backbone or other bases. For both 6MAP and DMAP, quench associated with going into an oligonucleotide is >90% and the decrease in $<\tau>$'s range from 43 to 71% for 6MAP and from 60% to 78% for DMAP. In those oligonucleotides experiencing a less severe decrease in $<\tau>$, the quenching mechanism can be attributed mostly to static interactions. In general, it appears that the DMAP probe is more subject to dynamic quenching than 6MAP since decreases in $<\tau>$ are consistently greater.

P1 Nuclease Digestion of 6MAP- or DMAP-Containing Single-Stranded Oligonucleotides

The P1 nuclease digestion of separate strands each containing one of the two probes, 6MAP and DMAP, demonstrates that the loss of fluorescence intensity (quench) for each probe as it is incorporated into DNA is caused by base interactions and not by degradation of the fluorophore resulting from the exposure to caustic chemicals during DNA synthesis. Figure 5 demonstrates how the quenching properties of these fluorophores can be used to display real time reactions as a protein causes a change in the structure of a strand (in this case, digestion) resulting in a constant increase in fluorescence intensity observable in real time.

T_m's of 6MAP- or DMAP-Containing Oligonucleotides

Melting temperatures provide another means for evaluating the behavior of these molecules within the structure of oligonucleotides. In previous experiments we determined that a blatant mismatch within the 21-base sequence pair used in the PTR series resulted in a 10°C depression of the melting temperature and that is approximately what was observed when measuring T_m's of 3MI-containing oligonucleotides (1). The adenosine analogs appear to be less disruptive of double-strand formation than 3MI. The T_m's listed in Table 3 are quite similar to the T_m of the control strands indicating that each of these two probes participates to some degree in base pairing. Table 4 shows the T_m results from pairing the two probes with each of the bases thymidine, adenosine, cytidine, or guanosine. The least perturbed pairing is achieved with thymidine for each 6MAP and DMAP, with T_m's in some cases very close to the T_m of the control strands.

CONCLUSIONS

These fluorophores, along with other fluorescent nucleoside analog, exhibit unique properties that make them extremely valuable for measuring subtle events within DNA. They are highly fluorescent, stable, and easy to use. Positioning one of these probes strategically within a strand of DNA may provide some indication of events occurring close to that site as reported directly by changes in fluorescence intensity, anisotropy, energy transfer, or lifetime measurements. Current projects in this lab are focusing on use of the probes to detect DNA hybridization without the need to separate products.

ACKNOWLEDGMENT

The authors thank Drs. Jay Knutson and John Harvey for help in measuring lifetimes and assistance in preparing the manuscript.

REFERENCES

1. Hawkins, M. E., Pfleiderer, W., Balis, F. M., Porter, D., and Knutson, J. R., (1997) Fluorescence properties of pteridine nucleoside analogs as monomers and incorporated into oligonucleotides. *Anal. Biochem.* **244,** 86–95.
2. Hawkins, M. E., Pfleiderer, W., Mazumder, A., Pommier, Y. G., and Balis, F. M., (1995) Incorporation of a fluorescent guanosine analog into oligonucleotides and its application to a real time assay for the HIV-1 integrase 3′-processing reaction. *Nucleic Acids Res.* **23,** 2872–2880.

3. Moser, A. M., Patel, M., Yoo, H., Balis, F. M., and Hawkins, M. E. (2000) Real-time fluorescence assay for O^6-alkylguanine–DNA alkyltransferase. *Anal. Biochem.* **281,** 216–222.
4. Wojtuszewski, K., Hawkins, M., Cole, J. L., and Mukerji, I., (2001) HU binding to DNA: Evidence for multiple complex formation and DNA bending. *Biochemistry* **40,** 2588–2598.
5. Lythgoe, G., Todd, A. R., and Topham, A., (1944) Experiments on the synthesis of purine nucleosides. V. The coupling of pyrimidine derivatives with diazonium salts: A method for the preparation of 5-aminopyrimidines. *J. Chem. Soc.* 315–317.
6. Pfleiderer, W. (1994) *in* Chemistry of Nucleosides and Nucleotides (Townsend, L. B., Ed.), pp. 214–255, Plenum, New York.
7. Birkofer, L., Ritter, A., and Kuhltau, G. P. (1964) Alkylierungen und glykosidierungen uber silyl-derivate. *Chem. Ber.* **97,** 934–945.
8. Birkofer, L., and Ritter, A. (1965) Die silylierung als hilfsmittel in der organischen synthese. *Angew. Chem.* **77,** 414–426.
9. Vorbruggen, H., and Hofle, G., (1981) On the mechanism of nucleoside synthesis. *Chem. Ber.* **114,** 1256–1268.
10. Jungmann, O., and Pfleiderer, W. (1996) New efficient method in nucleotide synthesis. *Tetrahedron Lett.* **37,** 8355–8358.
11. Zemplen, G., Geres, A., and Hadacsy, J. (1936) *Ber. Deut. Chem. Ges.* **69,** 1827.